CODEN:KDCHEW
ISSN 0916-0892

九州大学中央分析センター報告

― 第 30 号 ―

REPORT

OF

THE CENTER OF ADVANCED INSTRUMENTAL ANALYSIS

KYUSHU UNIVERSITY

NUMBER 30

2012

九州大学中央分析センター

－研　究　報　告－

Facile conjugation of porphyrin and N-confused porphyrin with nona-arginine peptide by click reaction

Yoshiya Ikawa*[1,2,3], Hiroyuki Harada1, Sho Katsumata[1], and Hiroyuki Furuta*[1,2]

[1] *Department of Chemistry & Biochemistry, Graduate School of Engineering, Kyushu University, 819-0395, Fukuoka, Japan*

[2] *Center for Molecular Systems, Kyushu University, 819-0395, Fukuoka, Japan*

[3] *Synthetic Systems Biology Research Center, Kyushu University, 812-8582, Fukuoka, Japan*

* Authors to whom correspondence should be addressed:
yikawa@cstf.kyushu-u.ac.jp; hfuruta@cstf.kyushu-u.ac.jp.

Abstract

Water-soluble derivatives of porphyrin (Por) and N-confused porphyrin (NCP) possessing a nona-arginine (R9) peptide tail were synthesized by Cu(I)-catalyzed azide-alkyne cycloaddition (click reaction). Acid-base properties of the two molecules were investigated in aqueous solutions. pH titration experiments revealed that the porphyrin-R9 conjugate molecule (**Por-R9**) undergoes a concerted diprotonation to generate dication from freebase whereas the NCP-R9 conjugate (**NCP-R9**) generates mono- and dication in a stepwise manner.

Keywords

porphyrin; N-confused porphyrin; click reaction; nona-arginine peptide

1. Introduction

Applications of porphyrin and related macrocycles (**Chart 1**) to biochemical/biomedical fields have attracted considerable attention because they are capable of interacting with biomacromolecules by the simple modification of the periphery to change hydrophobic macrocycles to hydrophilic. We have been interested in oligo-arginine peptides as an accessory moiety because they have been widely employed to afford water-solubility and cell-penetrating ability to a variety of hydrophobic molecules [1,2]. We recently succeeded in synthesizing a conjugated molecule of nona-arginine (R9) peptide and N-fused porphyrin (**NFP, Chart 1**), a porphyrin analogue having a unique [5.5.5] tripentacyclic structure embedded in a tetrapyrrolic macrocycle [3,4].

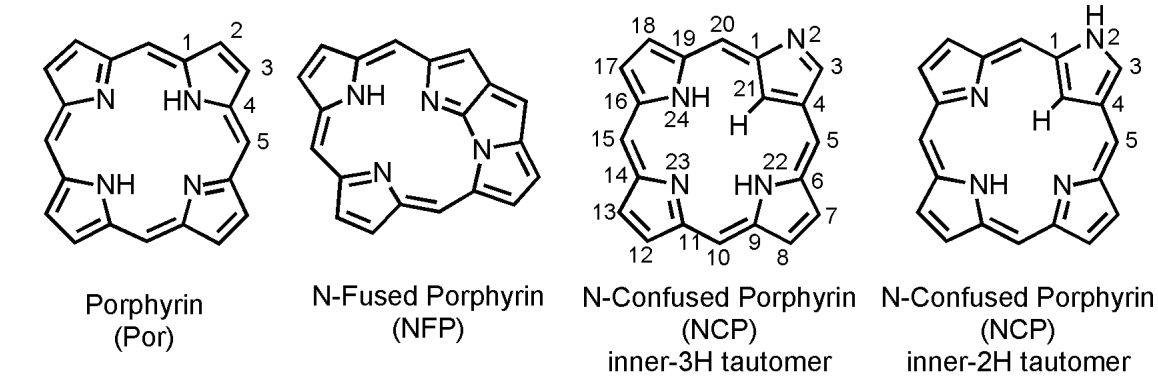

Chart 1. Basic structures of porphyrin, N-fused porphyrin, and two tautomers of N-confused porphyrin.

Conjugation of the R9 peptide with N-fused porphyrin was achieved by using Cu(I) catalyzed azide-alkyne Huisgen cycloaddition (click reaction) between an NFP derivative bearing an ethynyl moiety and a side-chain protected R9 peptide possessing an azide group at its *N*-terminus. The opposite terminus (C-terminus) of the protected, azide-modified R9 peptide was covalently attached to a solid support [4].

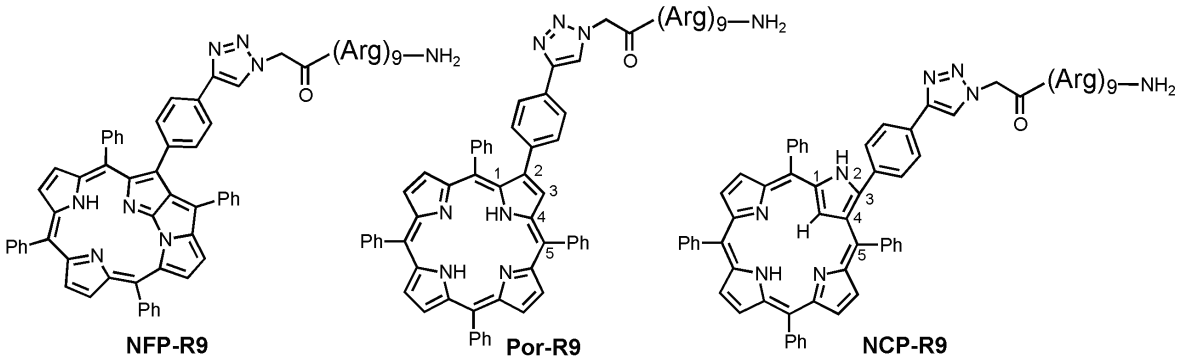

Chart 2. Conjugated molecules of nona-arginine (R9) peptide with N-fused porphyrn (**NFP-R9**), regular porphyrin (**Por-R9**), and N-confused porphyrin (**NCP-R9**).

An advantage of our synthetic strategy is easy handling and purification of the coupling product because it retains on the solid support after the reaction. Removal of the side-chain protecting groups and cleavage from the supported resin gave the target molecule (**NFP-R9, Chart 2**).

Since this synthetic strategy is practically useful, we decided to apply this strategy for conjugation of R9 peptide with other porphyrin-related macrocycles. We here report syntheses and basic properties of conjugated molecules of R9 peptide with regular porphyrin (**Por**) and N-confused porphyrin (**NCP**) [5], a porphyrin isomer possessing a confused pyrrole unit connected to the surrounding *meso*-carbons at the α- and β'-positions (**Chart 1**).

2. Results and Discussion

2.1. Syntheses of Por-R9 and NCP-R9 conjugates

To conjugate the azide-modified R9-peptide with porphyrin and N-confused porphyrin by click reaction, introduction of an ethynyl group to tetrapyrrolic macrocycles was required. We employed a phenylethynyl group as a building block for introduction of ethynyl moiety to tetrapyrrolic macrocycles because selective introduction of aryl groups to C2 position of porphyrin and C3 position of N-confused porphyrin has been achieved with cross-coupling reactions.

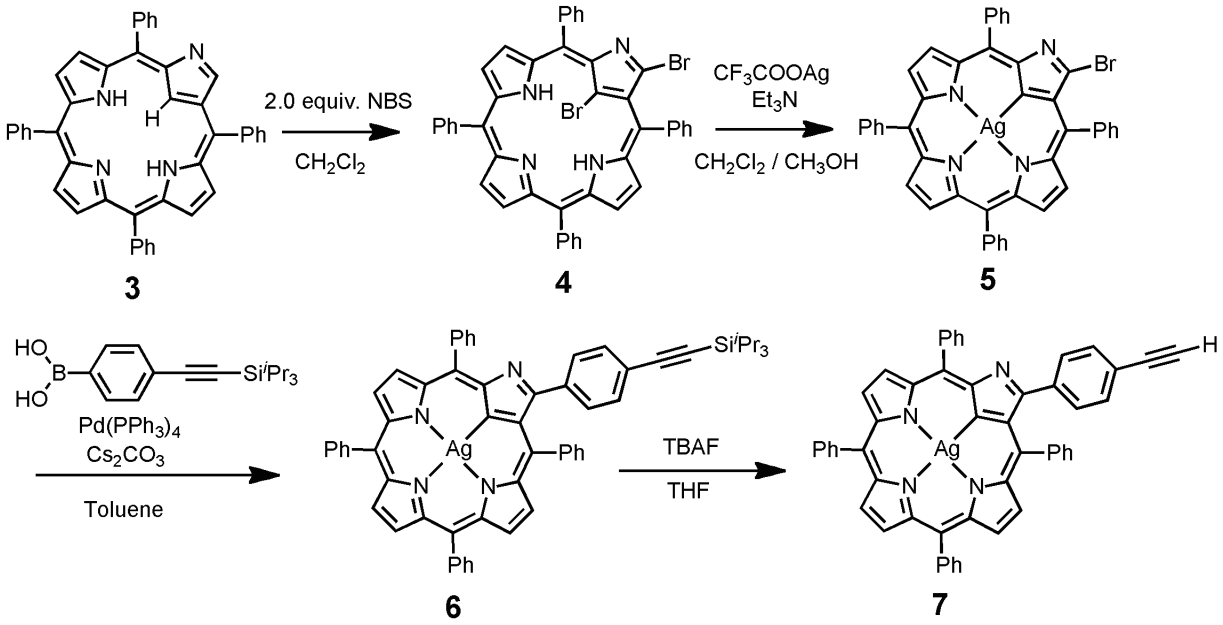

Scheme 1. Synthesis of an alkynated NCP derivative **7**.

Synthesis of a Zn(II) porphyrin possessing an ethynyl group (**2, Chart 3**) from tetraphenylporphyrin (TPP, **1**) has been reported [6]. We thus developed a synthetic route for an N-confused porphyrin derivative with an ethynyl group from a C3, C21-dibrominated NCP derivative (**Scheme 1**). Dibromo-NCP **4** was prepared by treating N-confused tetraphenylporphyrin (**NCTPP, 3**) with 2.0 equiv *N*-bromosuccinimide (NBS). Protection of the inner cavity of NCP skeleton and removal of bromine at C21 position were achieved simultaneously by treating **4** with CF_3COOAg to give a Ag(III) complex (**5**) [7]. 4-[(Triisopropylsilyl)ethynyl]phenyl moiety was then introduced at the C3 position of **5** by Pd(II)-catalyzed Suzuki cross-coupling in 51% to give **6**. Removal of the silyl protecting group of **6** by tetrabutylammonium fluoride (TBAF) proceeded quantitatively (99%) to give the desired NCP derivative (**7**) as a substrate for click reaction.

The side-chain protected nona-arginine (R9) peptide bearing an azidoglycine at the N-terminus (**Scheme 2**) was prepared by solid-phase peptide synthesis on Rink Amide resin as described previously [4]. The resulting N_3-Gly-$[Arg(Pbf)]_9$ peptide attached on the resin was coupled with porphyrin **2** or NCP **7** by Cu(I)-catalyzed cycloaddition between the azide moiety of the protected R9 peptide on the resin and the terminal alkyne in **2** or **7** (**Scheme 2**) [4]. The coupling reactions were carried out using CuI as Cu(I)-catalyst in CH_2Cl_2 under the reaction conditions developed for the synthesis of **NFP-R9**. After the coupling reaction, the resin was washed extensively with CH_2Cl_2 to eliminate excess **2** or **7**. The resulting resin was treated with a cleavage cocktail containing trifluoroacetic acid (TFA, v/v 90%), *m*-cresol (v/v 5%), and thioanisol (v/v 5%) to release the product from the resin and also to remove Pbf groups from arginine side-chains.

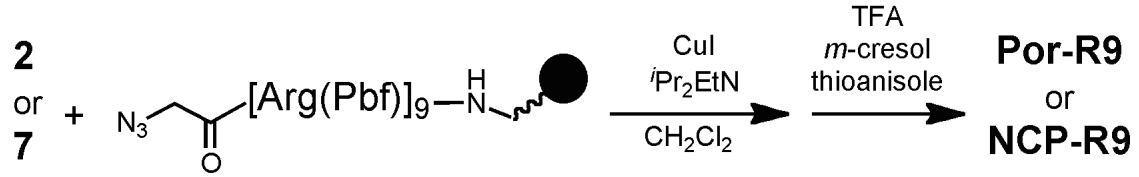

Scheme 2. Conjugation of R9 peptide with porphyrin **2** or NCP **7** by a Cu(I)-catalyzed alkyne-azide cycloaddition on the solid support, followed by acid cleavage from the resin. Pbf = 2,2,4,6,7-pentamethyldihydrobenzofuran-5-sulfonyl group.

Target molecules (**Por-R9** and **NCP-R9**) were purified with a reverse phase HPLC and stored as TFA salts. The target molecules were characterized by MALDI-TOF mass and UV-vis spectroscopy. As control molecules lacking the hydrophilic R9 peptide tail, compounds **8** and **9** (**Chart 3**) were synthesized by click reactions of **2** and **7** with ethyl azidoacetate, respectively.

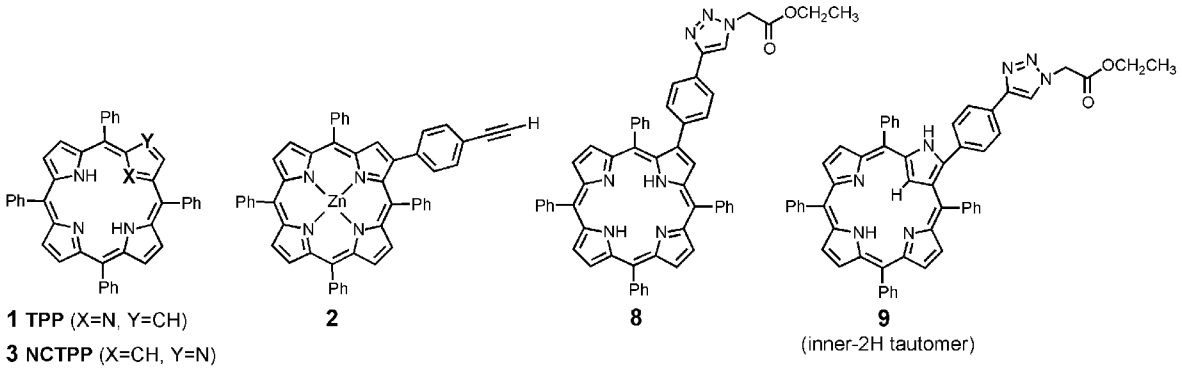

Chart 3.

Hydrophilic properties of **Por-R9** and **NCP-R9** were confirmed by partition experiments between H_2O and CH_2Cl_2. Nona-arginine conjugates (**Por-R9** and **NCP-R9**) selectively dissolved in H_2O while ethyl ester conjugates (**8** and **9**) were soluble only in CH_2Cl_2 (Fig. 1A).

*2.2. Photophysical and acid-base properties of **Por-R9***

The UV-vis absorption spectra of hydrophilic conjugates (**Por-R9** and **NCP-R9**) and hydrophobic controls (**8** and **9**) were measured in DMF (Figs. 1B and 1C). Absorption spectra of **Por-R9** and **NCP-R9** were closely similar to those of **8** and **9**, respectively, indicating that the nona-arginine (R9) moiety did not perturb absorption properties of the tetrapyrrolic skeletons (Figs. 1b and 1C). UV-vis absorption spectrum of **9** was also measured in CH_2Cl_2 (Fig. 1C) to evaluate the solvent-dependent NH tautomerism of the NCP skeleton in **NCP-R9** and NCP **9** (**Chart 1**) [8]. Soret-like band of **9** in CH_2Cl_2 was observed at 456 nm, which was 6 nm shorter than that in DMF (462 nm). Spectral shape of Q-like bands in CH_2Cl_2 (555, 597, and 755 nm) was also different from that in DMF (598 and 717 nm). Such solvent-dependent spectral changes of **9** resembled those of NCTPP (**3**), suggesting that NCP **9** and **NCP-R9** form the inner-2H tautomer in DMF whereas **9** dominantly exists as the inner-3H tautomer in CH_2Cl_2 [8].

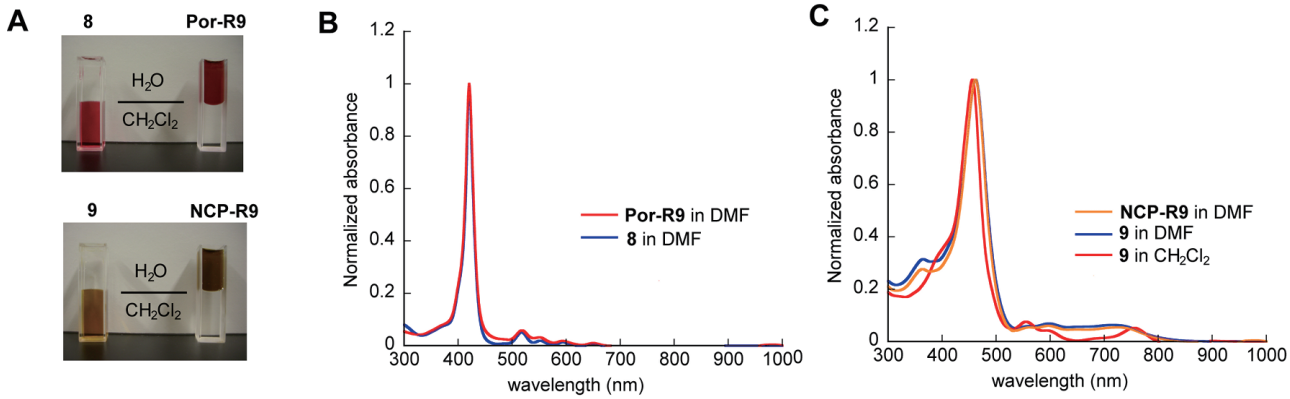

Figure 1. Partition experiments and UV-vis absorption spectra of hydrophilic and hydrophobic derivatives of porphyrin and N-confused porphyrin. (A) Partition experiments of **8** and **Por-R9** in H_2O+CH_2Cl_2 (top), and **9** and **NCP-R9** in H_2O+CH_2Cl_2 (bottom). (B) UV-vis absorption spectra of **Por-R9** and **8** in DMF. (C) UV-vis absorption spectra of **NCP-R9** in DMF and **9** in DMF and CH_2Cl_2.

UV-vis absorption spectra of **Por-R9** were then measured in aqueous media to evaluate its aggregation and acid-base properties. In ultrapure H_2O, addition of sodium dodecyl sulfate (SDS) caused no significant spectral change (data not shown), suggesting that **Por-R9** did not form strong aggregates in neutral H_2O solution. pH titration experiments were carried out using HCl and NaOH to adjust pH in acidic and basic regions, respectively (Fig. 2). With an increase of pH in the basic region, intensity of the Soret-band decreased. This result suggests that the aggregation of porphyrin skeleton took place under the basic conditions probably due to the charge neutralization of arginine side-chains in the R9 tail (Fig. 2A). Under acidic conditions, concerted protonation of two imine nitrogens was observed to generate the dication of **Por-R9** (Fig. 2B) and the pK value between the freebase and the dication was estimated to be 3.5.

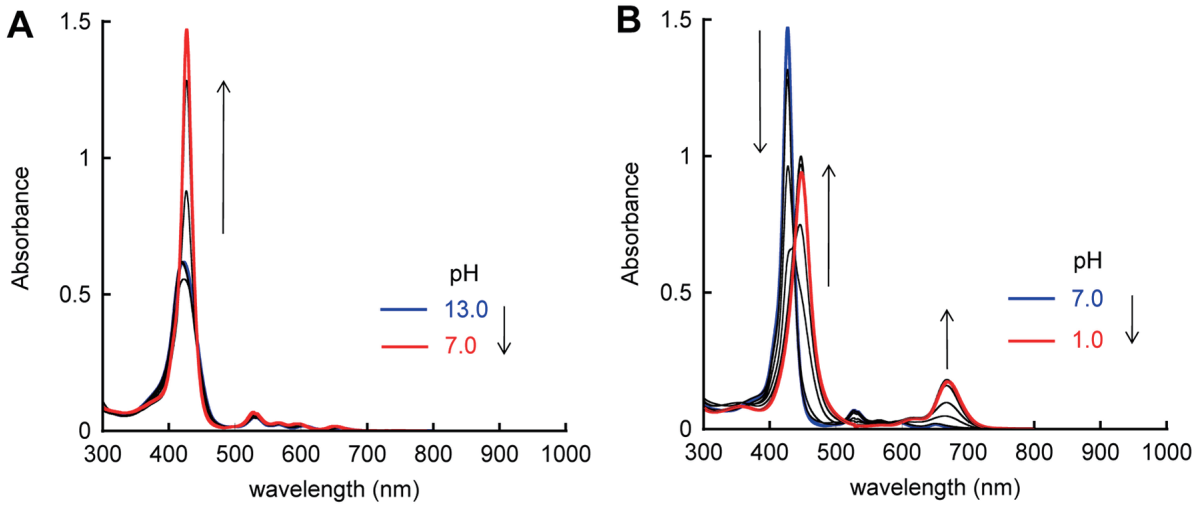

Figure 2. pH dependent spectral changes of **Por-R9** in ultrapure water, (A) between pH 13.0 and pH 7.0, and (B) between pH 7.0 and pH 1.0. Titrations were performed with aqueous NaOH and HCl. [**Por-R9**] = 10 μM.

*2.3. Photophysical and acid-base properties of **NCP-R9***

Two imine nitrogens in the NCP skeleton usually accept two protons in a stepwise manner owing to the structural asymmetry of the macrocycle. To confirm the absorption spectra of mono- and dication of NCP **9** in organic solvents we first measured the protonation behavior of NCP **9** in polar and nonpolar organic solvents (DMF and CH_2Cl_2). In DMF (which stabilizes the inner 2H-tautomer of **9**), addition of TFA caused two-step spectral changes corresponding to generation of mono- and diprotonated forms of **9** (Fig. 3A). Addition of 10 equiv TFA gave the monocation of **9** (**9•H**$^+$), whose absorption spectrum exhibited the Soret-like band at 471 nm and the broad Q-like bands reaching to 1000 nm. Addition of excess amount of TFA gave a new spectrum corresponding to the dication of **9** (**9•2H**$^+$). **9•2H**$^+$ had a Soret-like band with absorption maxima (λ_{max}) at 481 nm and three Q-like bands (620, 680, and 867 nm). Spectral profiles of **9•H**$^+$ and **9•2H**$^+$ were similar to the mono- and dication of a water-soluble NCP derivative having four pyridinium moieties in aqueous solution [9]. Two-step absorption spectral changes of **9** were also observed in CH_2Cl_2, in which **9** preferably formed the inner 3H-tautomer (Fig. 3B). Absorption spectrum of dication **9•2H**$^+$ in CH_2Cl_2 was similar to that in DMF. Soret-like bands of monocation **9•H**$^+$ in CH_2Cl_2 also had the λ_{max} (469 nm) that was similar to λ_{max} of **9•H**$^+$ in DMF (471 nm). On the other hand, a shape of Q-like bands of **9•H**$^+$ in DMF (Fig. 3B) was significantly different from that in CH_2Cl_2 (Fig. 3A), indicating that NCP **9** shows solvatochromic property not only in the freebase form but also in the monocationic form (**9•H**$^+$).

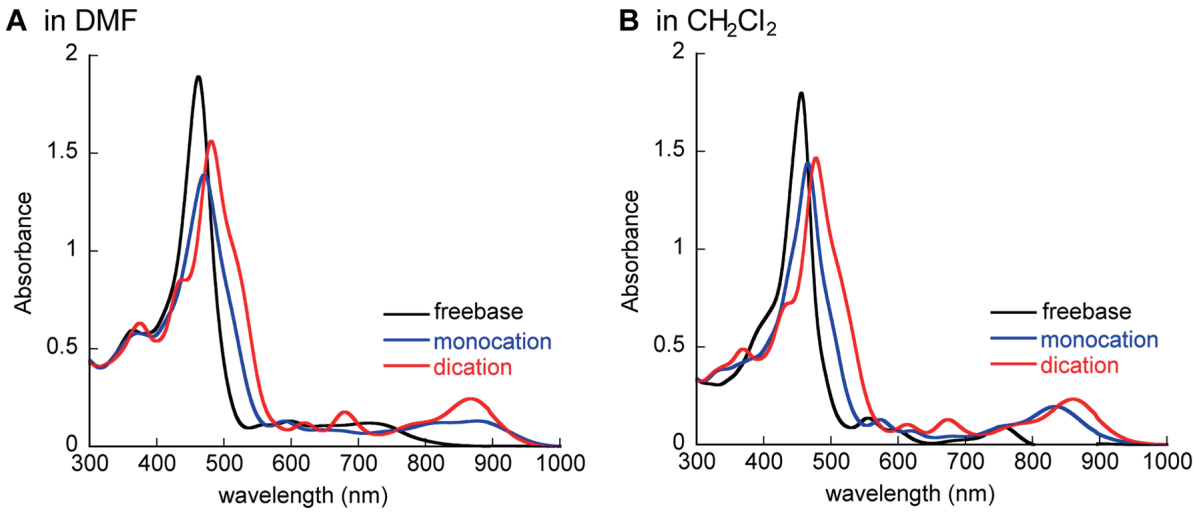

Figure 3. Protonation of **9** by TFA in DMF (A) and in CH_2Cl_2 (B).

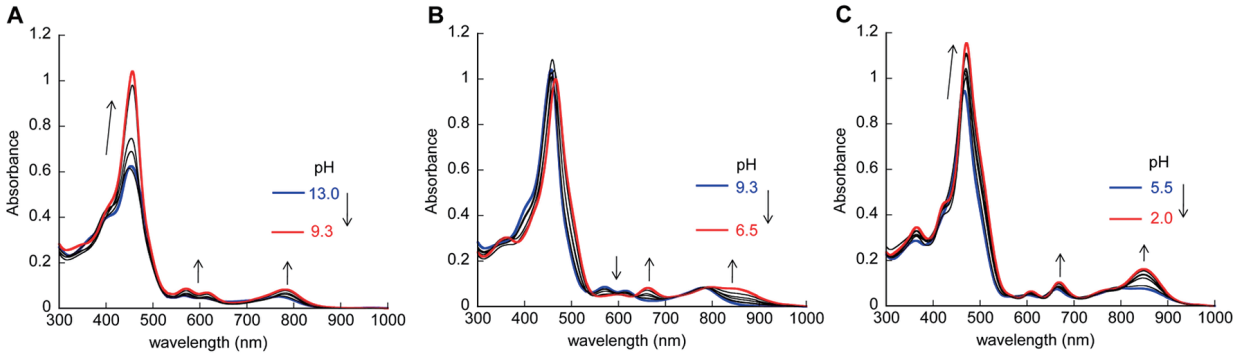

Figure 4. pH dependent spectral changes of **NCP-R9** in ultrapure water; (A) between pH 13.0 and pH 9.3, (B) between pH 9.3 and pH 6.5, and (C) between pH 5.5 and pH 2.0. Titrations were performed with aqueous NaOH and HCl. [**NCP-R9**] = 10 μM.

Acid-base property of **NCP-R9** was then investigated by adjusting pH of aqueous solution with HCl (acidic region) or NaOH (basic region). In the pH region between 9.3 and 13.0, intensity of the Soret-like band at 456 nm decreased with increasing pH (Fig. 4A), suggesting that **NCP-R9** formed the aggregates under the basic conditions. With a decrease of pH from 9.3 to 6.5, transition from the freebase to the monocation (**NCP-R9•H**$^+$) took place (Fig. 4B) because the absorption spectra of **NCP-R9** in pH 6.5-5.5, which showed a Soret-like band at 466 nm, were closely similar to that of **9•H**$^+$ in DMF. With a further decrease of pH from 5.5 to 2.0 (Fig. 4C), second transition was observed to generate the dication (**NCP-R9•2H**$^+$), spectral of which closely resembled **9•2H**$^+$. From the titration curve, the pK_a values of each protonation process, [**NCP-R9•2H**$^+$]//[**H+•NCP-R9•H**$^+$] and [**NCP-R9•H**$^+$]//[**NCP-R9**], were estimated to be 3.5 and 8.0, respectively. These pK_a values were comparable to those for **NCTPP** (**3**) measured in a 2.5% aqueous micellar SDS solution (3.27 for [**NCTPP•2H**$^+$]//[**NCTPP•H**$^+$], and 8.35 for [**NCTPP•H**$^+$]//[**NCTPP**]) [3, 10].

3. Perspective

We synthesized water-soluble conjugates of porphyrin and N-confused porphyrin with nona-arginine peptide (**Por-R9** and **NCP-R9**) by click reaction, and elucidated their basic absorption and acid-base properties. Syntheses and

elucidation of basic photophysical properties of these conjugates in this study allow us to apply them to biochemical/biomedical fields. An attractive direction for the application of **Por-R9** and **NCP-R9** is their use as therapeutic and/or diagnostic purposes. Generation of singlet oxygen inside living cells is an important property of porphyrin and related molecules. Owing to this property, water-soluble derivatives of porphyrin and related molecules are promising as photosensitisers for photodynamic therapy (PDT) [11]. Introduction of **Por-R9** and **NCP-R9** into cultured cells is possible without further modification because nona-arginine (R9) is a member of bioactive peptides with cell-penetrating ability. Investigation of their photophysical properties in cultured cells is currently ongoing in our group.

4. Materials and Methods

Materials and Methods

General: Commercially available reagents and solvents were used without further purification unless otherwise mentioned. THF was distilled over benzophenone and sodium under Ar atmosphere. Silica gel column chromatography was performed on KANTO Silica Gel 60 N (spherical, neutral, particle size 40—50 μm). ^{1}H NMR spectra were recorded on a JEOL JNM-AL300 spectrometer (operating 300.40 MHz for ^{1}H). Chemical shifts were expressed in parts per million (ppm) from a residual portion of deuterated solvent, $CHCl_3$ (δ = 7.26). MALDI-TOF-mass spectra were recorded on a Bruker Daltonics Autoflex with linear positive ion mode. UV-vis spectra were recorded on a Shimadzu UV-3150PC spectrometer. For UV-vis absorption measurements, spectroscopic grade solvents (DMF and CH_2Cl_2 purchased from Nacalai Tesque, Kyoto, Japan) and ultrapure water (prepared by Organo Puric-Z, Tokyo, Japan) were employed.

NCP 6: NCP 5 (400 mg, 0.50 mmol) [7], 4-[(triisopropylsilyl)ethynyl]phenylboronic acid (800 mg, 2.9 mmol), $Pd(PPh_3)_4$ (8 mg, 0.007 mmol), and Cs_2CO_3 (600 mg, 1.85 mmol) were dissolved in toluene (20 mL). The reaction mixture was stirred for 5 h under Ar at 90 ℃ . After removal of the solvent by evaporation, the residue was dissolved by a mixture of water–CH_2Cl_2, and the product was extracted with CH_2Cl_2. The organic phase was combined and dried over Na_2SO_4. After evaporation, the residue was separated by silica gel column chromatography with CH_2Cl_2 containing 1% MeOH. The second brown fraction afforded 250 mg of **6** (51%) as a brown solid. ^{1}H NMR ($CDCl_3$, 300 MHz, ppm): δ 1.21 (s, 21H), 7.19-7.25 (m, 2H), 7.28-7.41 (m 3H), 7.52 (d, 2H, J = 4.0 Hz), 7.64-7.86 (m, 11H), 8.07-8.18 (m, 4H), 8.26 (d, 2H, J = 4.0 Hz), 8.56-8.68 (m, 4H), 8.78 (d, 1H, J = 4.0 Hz), 8.88 (d, 1H, J = 4.0 Hz); MALDI-TOF-MASS: m/z = 976.883 [M^+].

NCP 7: NCP 6 (150 mg, 0.153 mmol) was dissolved in THF (15 mL). After adding tetrabutylammonium fluoride (1 M in THF) (62 mL, 0.23 mmol), the reaction mixture was stirred for 3 h under Ar at ambient temperature. After evaporation, the residue was recrystallized from CH_2Cl_2–MeOH. The brown crystal of 7 was obtained in a yield of 125 mg (99%). ^{1}H NMR (CDCl3, 300 MHz, ppm): δ 3.09-3.13 (s, 1H), 6.78-6.92 (m, 2H), 7.37-7.43 (m, 3H), 7.51-7.59 (d, 2H), 7.62-7.87 (m, 14H), 8.07-8.19 (s, 5H), 8.23-8.31 (d, 2H), 8.58-8.71 (m, 5H), 8.73-8.79 (d, 1H), 8.83-8.89 (d, 1H); MALDI-TOF-MASS: m/z = 819.370 [M^+].

Por-R9: Porphyrin 2 (78 mg, 0.1 mmol) [6] and CuI (19 mg, 0.1 mmol) were dissolved in CH_2Cl_2 (15 mL). After adding the peptide resin (approximately 0.05 mmol) and *N,N*-diisopropylethylamine (435 mL, 2.5 mmol), the mixture

was gently stirred for 12 h under Ar at ambient temperature. The resin was recovered by filtration and washed with CH_2Cl_2 five times. To cleave the peptide from the resin and remove Pbf groups, the resin was treated with a mixture of TFA (2.7 mL), *m*-cresol (150 mL), and thioanisole (150 mL) for 1 h at ambient temperature. After the resin was removed by filtration, diethyl ether (35 mL) was added to the solution to precipitate a crude compound as a green powder, which was collected by centrifugation. Three-twentyfifth of the crude compound was then purified by HPLC with YMC R-ODS-5 column (4.6 × 250 mm) using H_2O-CH_3CN mixed solvent containing 0.1% TFA. Stepwise gradient was employed; first 30% CH_3CN for 15 min, second 40% CH_3CN for 20 min, third 100% CH_3CN for 10 min; flow rate: 1 mL/min; detection: 220 nm (peptide), 420 nm (Porphyrin). The main peak eluted in 40 % CH_3CN was collected and lyophilized to afford 1.4 mg of a green powder (0.431 μmol as **Por-R9**•9CF_3COO^-, 7.17% yield from 2.5 μmol Fmoc-Rink Amide resin). MALDI-TOF-MASS: *m/z* = 2221.07 [M^+].

NCP-R9: NCP 6 (82 mg, 0.1 mmol) and CuI (19 mg, 0.1 mmol) were dissolved in CH_2Cl_2 (15 mL). After adding the peptide resin (approximately 0.05 mmol) and DIPEA (435 mL, 2.5 mmol), the mixture was gently stirred for 12 h under Ar at ambient temperature. The resin was recovered by filtration and washed with CH_2Cl_2 five times. To cleave the peptide from the resin and remove Pbf groups, the resin was treated with a mixture of TFA (2.7 mL), *m*-cresol (150 mL), and thioanisole (150 mL) for 1 h at ambient temperature. After the resin was removed by filtration, diethyl ether (35 mL) was added to the solution to precipitate a crude compound as a brown powder, which was collected by centrifugation. One-twentieth of the crude compound was then purified by HPLC with YMC R-ODS-5 column (4.6 × 250 mm) using H_2O-CH_3CN mixed solvent containing 0.1% TFA. Stepwise gradient was employed; first 30% CH_3CN for 10 min, second 40% CH_3CN for 20 min, third 100% CH_3CN for 10 min; flow rate: 1 mL/min; detection: 220 nm (peptide), 450 nm (NCP). The main peak (**NCP-R9**) eluted in 40% CH_3CN was collected and lyophilized to afford 0.5 mg of a brown powder (0.154 μmol as **NCP-R9**•9CF_3COO^-, 6.1% yield from 2.5 μmol Fmoc-Rink Amide resin). MALDI-TOF-MASS: *m/z* = 2222.31 [M^+].

NCP 9-Ag(III) complex: NCP 7 (100 mg, 0.123 mmol) and CuI (46 mg, 0.246 mmol) were dissolved in CH_2Cl_2 (10 mL). After adding ethyl azidoacetate (317 mL, 2.46 mmol) and DIPEA (1074 mL, 6.15 mmol), the mixture was stirred for 12 h under Ar at ambient temperature. After removal of the solvent by evaporation, the residue was dissolved in a mixture of water–CH_2Cl_2, and the product was extracted with CH_2Cl_2. The organic phase was combined and dried over Na_2SO_4. After evaporation, the residue was separated by silica gel column chromatography with CH_2Cl_2 containing 1% MeOH. The first brown fraction afforded 75 mg of **NCP 9-Ag(III) complex** (64%) as a brown solid. ^{1}H NMR ($CDCl_3$, 300 MHz, ppm): δ 1.37 (t, 3H), 4.35 (q, 2H), 5.26 (s, 2H), 7.4-7.55 (m, 1H), 7.58-7.69 (m, 5H), 7.69-7.81 (m, 10H), 7.86 (d, 1H, *J* = 4.8 Hz), 7.93 (s, 1H), 8.09-8.19 (m, 5H), 8.28 (d, 2H, *J* = 4.0 Hz), 8.57-8.69 (m, 4H), 8.78 (d, 2H, *J* = 4.0 Hz), 8.89 (d, 2H, *J* = 4.0 Hz); MALDI-TOF-MASS: *m/z* = 949.256 [M^+].

NCP 9: NCP 9-Ag(III) complex (50 mg, 0.053 mmol) was dissolved in CH_2Cl_2 (5 mL). After adding 1.0 mL TFA, the mixture was stirred for 2 h at ambient temperature. After removal of the solvent by evaporation, the residue was dissolved by a mixture of water–CH_2Cl_2 and neutralized with $NaHCO_3$. The product was extracted with CH_2Cl_2 and the organic phase was combined and dried over Na_2SO_4. After evaporation, the residue was separated by silica gel column chromatography with CH_2Cl_2 containing 1% MeOH. The third brown fraction afforded 21 mg of **NCP 9** (47%) as a

brown solid. ^{1}H NMR ($CDCl_3$, 300 MHz, ppm): δ -4.51 (s, 1H), 1.34 (t, 3H), 4.31 (q, 2H), 5.2 (s, 2H), 7.32 (d, 1H, J = 4.0 Hz), 7.4–7.48 (m, 2H), 7.53 (s, 5H), 7.72–7.82 (m, 8H), 7.82-7.94 (m, 3H), 8.14 (s, 4H), 8.26 (d, 2H, J = 8.0 Hz), 8.32-8.4 (m, 3H), 8.43 (d, 1H, J = 4.0 Hz), 8.49 (d, 1H, J = 8.0 Hz), 8.80 (d, 1H, J = 4.0 Hz), 8.87 (d, 1H, J = 4.0 Hz); MALDI-TOF-MASS: m/z = 841.064 [M^+].

5. Acknowledgement

This work is supported by Grants-in-Aids for Challenging Exploratory Research (No.23655159 to Y.I.), on Innovative Areas “Emergence in Chemistry” (No.21111518 to Y.I.) and “Emergence of highly elaborated π-space and its function” (No. 21108518 to H.F.) from the Ministry of Education, Culture, Sports, Science and Technology (MEXT), Japan.

6. References

1. Fuchs, S. M.; Raine, R. T. *Biochemistry*, **2004**, *43*, 2438.
2. Langel, Ü. *Handbook of Cell-Penetrating Peptides 2nd Ed.*; Taylor & Francis, Boca Raton, **2002**.
3. Furuta, H.; Ishizuka, T.; Osuka, A.; Ogawa, T. *J. Am. Chem. Soc*. **2000**, *122*, 5748.
4. Ikawa, Y.; Harada, H.; Toganoh, M.; Furuta, H. Bioorg. *Med. Chem. Lett*. **2009**, *19*, 2448.
5. Furuta, H.; Asano, T.; Ogawa, T. *J. Am. Chem. Soc*. **1994**, *116*, 767.
6. Toganoh, M.; Harada, H.; Ikawa, Y.; Furuta, H. *Chem. Lett*. **2010**, *39*, 252.
7. Ishizuka, T.; Yamasaki, H.; Osuka, A.; Furuta, H. *Tetrahedron* **2007**, *63*, 5137.
8. Furuta, H.; Ishizuka, T.; Osuka, A.; Dejima, H.; Nakagawa, H.; Ishikawa, Y. *J. Am. Chem. Soc*. **2001**, *123*, 6207.
9. Ikawa, Y.; Moriyama, S.; Harada, H.; Furuta, H. *Org. Biomol. Chem*. **2008**, *6*, 4157.
10. Ikawa, Y.; Ogawa, H.; Harada, H.; Furuta, H. *Bioorg. Med. Chem. Lett.* **2008**, *18*, 6394.
11. Josefsen, L. B.; Boyle, R. W. *Theranostics*, **2012**, *2*, 916.